Geoderma 213 (2014) 312–319

Contents lists available at ScienceDirect

Geoderma

journal homepage: www.elsevier.com/locate/geoderma

An evaluation of digital elevation models (DEMs) for delineating land components

Zama Eric Mashimbye [a,b,*], Willem Petrus de Clercq [a], Adriaan Van Niekerk [b]

[a] Department of Soil Science, Stellenbosch University, Private Bag X1, Matieland 7602, South Africa
[b] Department of Geography and Environmental Studies, Stellenbosch University, Private Bag X1, Matieland 7602, South Africa

ARTICLE INFO

Article history:
Received 25 January 2013
Received in revised form 29 July 2013
Accepted 19 August 2013
Available online xxxx

Keywords:
Digital soil mapping
Object-based image analysis
Land components
Multi-scale digital terrain analysis
Terrain units

ABSTRACT

Land component boundaries often coincide with transitions in environmental land properties such as soil, climate and biology. Image segmentation is an effective method for delineating terrain morphological units from digital elevation models (DEMs). This paper compares the land components derived from five DEMs. The second version of the 30-m advanced spaceborne thermal emission and reflection radiometer global DEM (ASTER GDEM2), the 90-m shuttle radar topography mission DEM (SRTM DEM), two versions of the 5-m Stellenbosch University DEMs (SUDEM L1 and L2) and a 5-m DEM (GEOEYE DEM) derived from GeoEye stereo-images were considered. The SRTM DEM and the ASTER GDEM2 were upsampled to 5-m resolution for comparison purposes. Land components were delineated using the slope gradient and aspect derivatives of each DEM. The resulting land components were visually inspected and quantitatively analyzed using the slope gradient standard deviation (SGSD) measure and the mean slope gradient local variance (MSGLV) ratio. The results show that the GEOEYE DEM and SUDEM L2 yielded land components with relatively low SGSD values and that their boundaries often coincide with morphological discontinuities. The GEOEYE DEM produced land components with the highest MSGLV ratio, followed by SUDEM L2, ASTER GDEM2, SRTM DEM and SUDEM L1. Although the land components derived from SRTM DEM and SUDEM L1 were relatively homogeneous internally, their boundaries did not always trace morphological discontinuities. The ASTER GDEM2 failed to incorporate many of the morphological discontinuities in the study area. It is concluded that, although the SRTM DEM is more suitable than the ASTER GDEM2 for generating land components, higher-resolution DEMs such as the GEOEYE DEM and SUDEM L2 are required for delineating meaningful land components.

1. Introduction

Terrain is one of the most important soil-forming factors (Behrens et al., 2010; Jenny, 1941) and is essential for soil property mapping (McBratney et al., 2003). According to Moller et al. (2008), landforms and landscape context are particularly import to understanding the processes of soil genesis and soil formation in the spatial domain. Minár and Evans (2008) describe land components as landform elements with a constant value of elevation or having a constant value of two or more readily interpretable morphometric variables, bordered by lines of discontinuities. Land component borders frequently coincide with environmental land properties such as soil, climate and biology (MacMillan et al., 2004; Speight, 1977; Van Niekerk, 2010).

Conventional approaches to delineating land components include studying topographical maps, interpreting aerial photographs and making field measurements (Drăguţ and Blaschke, 2006; Graff and Usery, 1993; Speight, 1977). However, these methods are often time-consuming, biased and costly (Adediran et al., 2004; Argialas, 1995; Drăguţ and Blaschke, 2006; Speight, 1977; Van Niekerk, 2010). The increasing availability of DEMs has promoted the use of computers and image processing techniques for deriving terrain properties. The application of object-based image analysis for land component mapping has gained popularity in recent years (Drăguţ and Blaschke, 2006; Drăguţ and Eisank, 2011; Smith et al., 2007; Wulder et al., 2008), particularly for soil-landscape modeling purposes (Blaschke and Stobl, 2003; Deng, 2007).

Various researchers have investigated the use of DEMs for digital soil and land component mapping. Van Niekerk (2010) evaluated land component maps delineated from DEMs using three algorithms, namely the automated land component mapper (ALCoM), the iterative self-organizing data analysis technique algorithm (ISODATA) and multi-resolution image segmentation (MRS) to determine which technique yields the most homogenous and morphologically representative land components. The three algorithms generated significantly different land component maps and MRS performed better and was more sensitive to morphological discontinuities than the other algorithms. Drăguţ and Blaschke (2006) investigated an automated classification system of landform elements based on object-orientated image analysis. Elevation, profile curvature, plan curvature and slope gradient was used to

* Corresponding author at: Private Bag X79, Pretoria 0001, South Africa. Tel.: +27 12 310 2576; fax: +27 12 323 1157.
E-mail address: mashimbyee@arc.agric.za (Z.E. Mashimbye).

0016-7061/$ – see front matter © 2013 Elsevier B.V. All rights reserved.
http://dx.doi.org/10.1016/j.geoderma.2013.08.023

delineate relatively homogeneous objects through image segmentation. This was followed by a classification of objects into landform elements using a relative classification model based on the surface shape and on the altitudinal position of objects. They concluded that the methodology is reproducible and it is readily adaptable for diverse landscapes and data sets. A semi-automated method to recognize and spatially delineate geomorphological units in mountainous forested ecosystems using statistical information extracted from a 1-m resolution digital terrain model (DTM) derived from laser data was proposed by van Asselen and Seijmonsberen (2006). They determined slope angle and elevation characteristics for each key geomorphological unit occurring in the study area and derived a map of slope classes from the DTM in an expert-driven multilevel object-orientated approach. They concluded that topographical data derived from high-resolution DTMs are useful for the extraction of geomorphological units in mountainous areas.

It has been demonstrated that delineating land components from DEMs is more cost-effective and objective than traditional field-based and visual interpretation methods and that land component mapping is invaluable for landscape characterization and soil mapping (Minár and Evans, 2008; Moller et al., 2008). However, although research has been done on the various algorithms available for segmenting DEMs to produce land components (Van Niekerk, 2010), very little has been done to determine how the use of different input DEMs influences the delineation of land components. This paper compares the land components derived from five DEMs, namely the 90-m shuttle radar topography mission DEM (SRTM DEM), the second version of the 30-m advanced spaceborne thermal emission and reflection radiometer global digital elevation model (ASTER GDEM2), two versions of the 5-m Stellenbosch University DEM (SUDEM L1 and L2), and a 5-m DEM (GEOEYE DEM) derived from GeoEye stereo-images. The results are interpreted and evaluated in the context of using land component delineation for mapping and studying soil properties.

2. Materials and methods

2.1. Study area

The Sandspruit catchment, a subcatchment in the Berg River basin, was chosen as the study area. The catchment has an extent of 152 km^2 and is situated in the vicinity of Riebeek-Wes, north of Cape Town in the Western Cape Province of South Africa (Fig. 1). The geology of the Sandspruit catchment is dominated by Malmesbury shales, although there are smaller occurrences of fine sediment, silcrete–fericrete, greenstone, quartzite and granite. Most of the catchment is used for dryland cultivation, particularly winter wheat. Land is also used for canola cultivation and pasturage. Natural vegetation covers only a small proportion of the catchment.

The Sandspruit catchment has a semi-arid (Mediterranean) climate and is located in a winter rainfall region with a mean annual rainfall of about 400 mm (Flügel, 1995). The catchment generally has undulating topography with gentle to moderate slopes. According to Flügel (1995), the valleys have a molded shape and the groundwater table is shallow in the lower-lying areas during the winter rainfall season. Salt crystallizes in patches during the hot summers from November to March. The Sandspruit catchment was considered a suitable site for this study as its landforms are representative of large parts of the Berg River catchment.

2.2. Data

2.2.1. Digital aerial photographs

High resolution (0.5 m) orthorectified digital aerial images covering the Sandspruit catchment were obtained from the Chief Directorate National Geo-spatial Information (CDNGI) (http://www.ngi.gov.za). The orthorectified digital aerial images were used to delineate test morphological discontinuities and as backdrops when assessing the accuracy of the DEM-delineated land components.

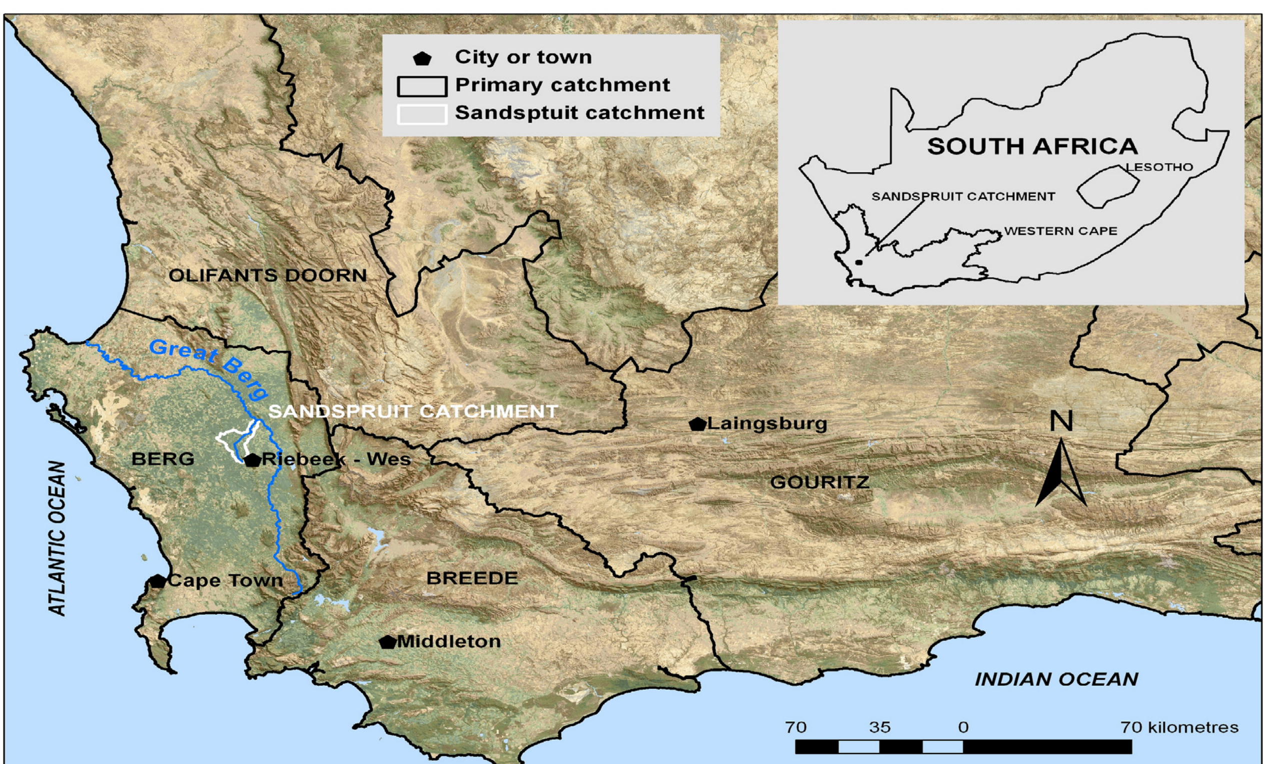

Fig. 1. Location of the Sandspruit catchment.

2.2.2. DEMs

A survey of available DEMs revealed that six DEMs were available for the study area; namely the 90-m SRTM DEM (http://srtm.csi.org), the 30-m ASTER GDEM2 (http:www.gdem.ersdac.or.jp), two versions of the 5-m SUDEM (http://www.sun.ac.za/cga), the 25-m CDNGI DEM (http://www.ngi.gov.za), the 20-m Western Cape digital elevation model (WCDEM) (http://www.sun.ac.za/cga) and the 30-m DEM developed by ComputaMaps (http://www.computamaps.com). Additionally, a 5-m GEOEYE DEM was generated from GeoEye stereo-images. Each DEM is described in the subsequent subsections.

2.2.2.1. SRTM DEM. The 90-m SRTM DEM, completed in 2000, is the first high-resolution DEM developed at near-global scale (Farr and Kobrick, 2001; Li and Wong, 2010). The SRTM DEM is reported to have a vertical error of less than 16 m (Farr, 2000; Mulder et al., 2011; Rodriguez et al., 2005; Van Niekerk, 2008). According to the Consultative Group on International Agricultural Research Consortium for Spatial Information (CGIAR-CSI, 2011), the latest version of the SRTM DEM has been processed to fill data voids and it is suited to a range of potential users.

2.2.2.2. ASTER DEM. The ASTER GDEM was developed jointly by the Ministry of Economy, Trade and Industry (METI) of Japan and the United States National Aeronautics and Space Administration (NASA). The full 1.5-million-scene ASTER archive was used to create the DEM. The second version of ASTER GDEM (GDEM2) was released in October 2011 (ASTER GDEM Validation Team, 2011) with the inclusion of 26,000 additional scenes to improve coverage. A smaller correlation kernel was also used to yield higher spatial resolution and enhanced water masking. ASTER GDEM2 was validated by comparing it to the absolute geodetic references over the conterminous United States (CONUS), the national elevation grids over the US and Japan, the SRTM 1 arc-second DEM over the US and 20 sites around the globe, as well as global space-borne laser altimeter data. The vertical and horizontal accuracies of the GDEM2 are less than 17 m and 71 m respectively (ASTER GDEM Validation Team, 2011; Mukherjee et al., 2013). The number of voids and artifacts noted in GDEM1 were substantially reduced in GDEM2 and were almost eliminated in some areas (ASTER GDEM Validation Team, 2011).

2.2.2.3. GEOEYE DEM. The GEOEYE DEM was created from GeoEye stereo-images acquired in July 2011. As with the ASTER GDEM, the elevation data that were extracted from the GeoEye imagery included objects above ground (i.e. it is a surface model and not a terrain model). However, because most of the study area is used for cultivation of grains, very few tall objects (e.g. trees and buildings) are present. Moreover, the July images record a time when the crops were at seedling height and thus had very little impact on the extracted elevations. Elevations were extracted at a 5-m horizontal interval using the rational polynomial coefficients (RPC) model in the LPS module of Erdas Imagine software. The resulting GEOEYE DEM was validated using the altitudes at reference points (trigonometric beacons) in the Sandspruit catchment. An absolute vertical accuracy of 0.70 m was achieved. The DEM was smoothed with a 7 × 7 circular median filter to remove artifacts caused by vegetation and crop patterns. Judging by the visual inspection of histograms (Fig. 2) prior to and after the filtering, and the attributes recorded in Table 1, the filter did not significantly alter the terrain morphology.

2.2.2.4. SUDEM. The SUDEM was developed by the Centre for Geographical Analysis (CGA) at Stellenbosch University, South Africa. Large-scale (1:10,000) contours and spot heights were used to interpolate two DEM products (Van Niekerk, 2011) using a combination of interpolation algorithms (e.g. the Topo to Raster and Spline tools in ArcGIS software). The first product (Level 1) only used 5-m vertical interval contours and spot heights as input, whereas the second product (Level 2) combined contours, spot heights and the SRTM DEM ("research-grade" version). For Level 2, the SRTM DEM was used to supplement the contour and spot height data in areas of low relief (i.e. where contour and spot height density was low). Contours are not ideal for interpolating DEM as their densities vary with slope gradient. Areas of low relief are particularly problematic as contours are often spaced far apart (horizontally) reducing the reliability of interpolations in such areas. To alleviate the problem of low contour densities in areas of moderate terrain, additional spot heights are often shown at strategic locations on topographical maps. Although the quality of a DEM can be improved by incorporating these elevation points in the interpolation process, the combined density of input points (i.e. contour vertices and spot heights) is often insufficient to represent subtle changes in terrain (e.g. floodplains and river banks), particularly in flat areas where input points can be several kilometers apart. In addition, contours digitized from topographical maps are generalizations of terrain and consequently exclude much of the variation that is often apparent in regularly sampled elevation sources such as the SRTM DEM. Experiments showed

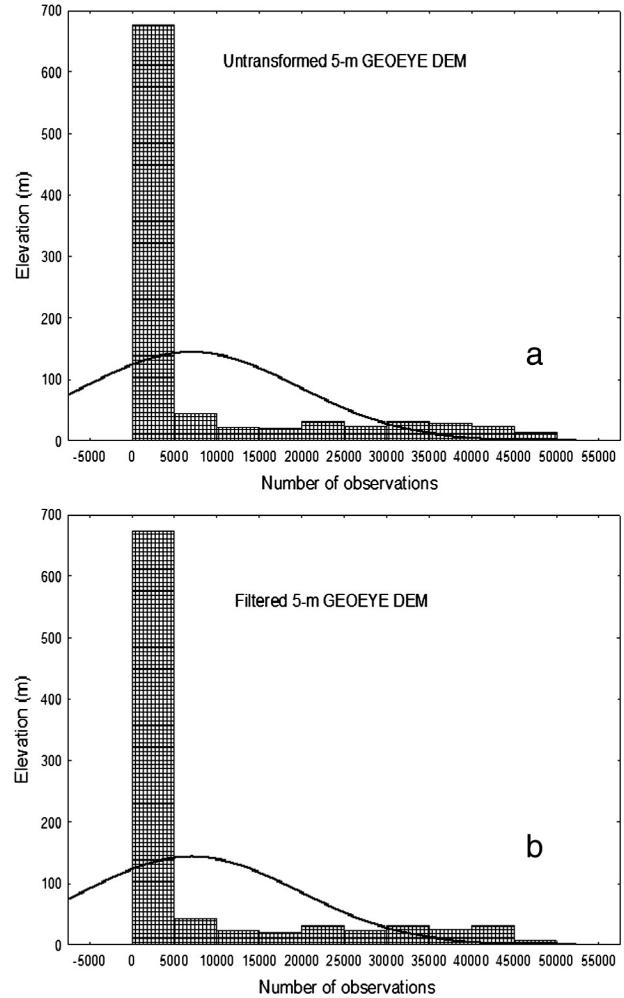

Fig. 2. Histograms showing the distribution of elevation values for the Sandspruit catchment using (a) the untransformed GEOEYE DEM and (b) filtered GEOEYE DEM.

Table 1
Attributes of original and filtered 5-m GEOEYE DEM.

DEM attributes	Original GEOEYE DEM	Filtered GEOEYE DEM
Minimum elevation (m)	34	34
Maximum elevation (m)	944	940
Mean elevation (m)	167.6	167.6
Standard deviation	82.6	82.6

GEOEYE DEM — digital elevation model created from GeoEye stereo images.

that, in spite of the relatively low resolution (90 m) and low vertical accuracy (16 m) of the SRTM DEM, significant improvements in absolute and relative vertical accuracies can be achieved when the SRTM DEM is used in combination with contours and elevation points in relatively flat areas (Van Niekerk, 2012).

2.2.2.5. Other available DEMs not used. The 25-m CDNGI DEM, the 20-m WCDEM and the 30-m DEM developed by ComputaMaps were not included in this study. The WCDEM and the ComputaMaps DEM were created from small scale-contours (1:50,000) and were expected to contain less detail than the SUDEM products. The CDNGI DEM was not used because it includes irregularities such as striping and seaming. This DEM reportedly has variable quality which could produce artifacts and unrealistic values when used to derive slope gradient and slope aspect (Thompson et al., 2001; Van Niekerk, 2008).

2.3. Data preparation

All the DEMs were projected to the Universal Transverse Mercator projection (Zone 34S). For easier comparison, the SRTM DEM and ASTER GDEM2 were upsampled from their native resolutions (90 and 30 m respectively) to 5-m resolution. This was achieved by converting the DEMs to points and interpolating new elevation values using the default settings of the Spline (tension) algorithm in ArcGIS 9.3 software. It is evident from Fig. 3 and Table 2 that the upsampling did not significantly alter the data content of the original DEMs. The histograms for the upsampled and original DEMs showed comparable distributions of slope gradient percentage prior to and following the upsampling procedure (Fig. 3a–d).

2.4. Land component segmentation

Land component segmentation was carried out using the MRS algorithm as implemented in eCognition 8.6 software (http://www.ecognition.com). The MRS algorithm is a bottom–up segmentation algorithm based on a pairwise region-merging technique (Blaschke, 2010; Mathieu et al., 2007). According to Trimble (2011), the segmentation procedure starts with single image object of one pixel and repeatedly merges them in several loops in pairs to larger units as long as an upper threshold of homogeneity is not exceeded. In the first step of the procedure the seed looks for its best-fitting neighbor for a potential merger and if best fitting is not mutual, the best candidate image object becomes the new seed image object and is fitted with its best partner. When best fitting is mutual, image objects are merged. In each loop every image object in the image object level is handled once. The loops continue until no further merger is possible (Mancas et al., 2005; Thakur and Anand, 2005; Trimble, 2011; Van Niekerk, 2010).

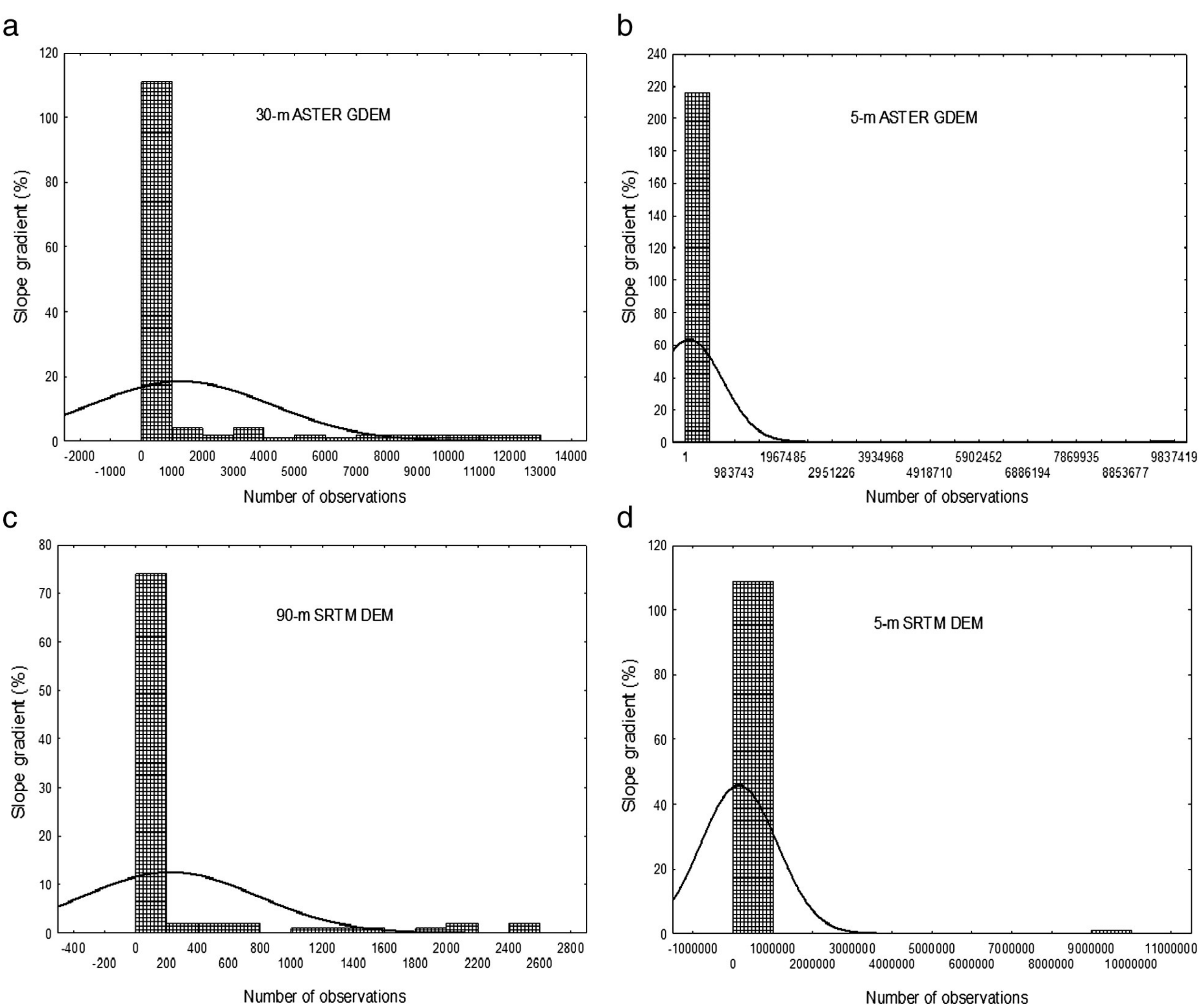

Fig. 3. Histograms showing the distribution of slope gradient percentage using the (a) original 30-m ASTER GDEM, (b) 5-m upsampled ASTER GDEM, (c) original 90-m SRTM DEM and (d) 5-m upsampled SRTM DEM for the Sandspruit catchment.

Table 2
Attributes of original and upsampled ASTER GDEM and SRTM DEM.

DEM attributes	90-m SRTM	5-m SRTM	30-m ASTER GDEM	5-m ASTER GDEM
Minimum elevation (m)	41	40	25	24
Maximum elevation (m)	928	919	935	935
Mean elevation (m)	170.1	167.3	161.5	161.1
Standard deviation	87.8	79.7	81.4	81.6

ASTER GDEM2 — second version of the 30-m advanced spaceborne thermal emission and reflection radiometer global digital elevation model and SRTM DEM — the 90-m shuttle radar topography mission digital elevation model.

Slope gradient and slope aspect were used as input layers to MRS for the detection of boundaries of land components. According to Minár and Evans (2008), the changes in the values of boundary-defining properties give the precise sharpness of the boundary. Slope aspect was converted to mean vector strength for analysis. A suitable MRS scale factor was determined by experimentation and visual interpretation using hill-shaded DEMs as backdrops (Drăguţ et al., 2011; Van Niekerk, 2010). A systematic approach was used by increasing the scale factor by one until meaningful objects were obtained (Drăguţ et al., 2010). This experimentation with suitable scale factors was carried out on the DEM with the highest detail (i.e. GEOEYE DEM). The MRS algorithm was configured by setting the shape parameter to its minimum value (0.1) and color was set to its maximum value (0.9) to maximize the internal homogeneity of objects. Both input layers were allocated equal weights in the segmentation. For the GEOEYE DEM, a scale factor of 12 produced land components that best represented terrain morphology of the study area. The scale factors for the other DEMs were adjusted so that their segmentations yielded a similar number of objects to allow comparison. The incorporation of plan and profile curvature as input to MRS was investigated, but this produced a large number of very small land components. This was attributed to the observation that changes in profile curvature often occur near slope gradient breaks. The combination of profile curvature and slope gradient reduced the ability of MRS to delineate land components along significant terrain discontinuities. The parameters and the number of objects produced by all the DEMs are summarized in Table 3.

2.5. Land component evaluation

Three assessment methods were employed to evaluate the land components delineated from each of the DEMs. First, the land components were visually inspected using hill-shaded DEMs and contours as backdrops. Visual interpretation entailed evaluating how well the land components identified morphological discontinuities (e.g. aspect and slope breaks). The second assessment method evaluated the internal homogeneity of the land components by computing the mean SGSD (Van Niekerk, 2010). It was premised that a small SGSD is indicative of high internal homogeneity (i.e. low interclass differences) and that a higher proportion of units with small SGSDs suggests accurate land component delineation (Van Niekerk, 2010). The third assessment method employed the mean slope gradient local variance (MSGLV) to determine the effectiveness of the derived land components to detect morphological discontinuities (i.e. high interclass difference). Given that local variance (LV) is the mean of the standard deviation (SD) computed in a small neighborhood (usually a 3×3 moving window) (Drăguţ and Eisank, 2011; Drăguţ et al., 2011), a satisfactory land component delineation will maximize internal (interclass) homogeneity and minimize external (intraclass) homogeneity. A land component should ideally have a low internal MSGLV and a high MSGLV at its edges. In this study the land component boundaries were defined as being one pixel (5 m) in width and all other pixels were considered internal. Internal and edge MSGLV were calculated for each set of land components derived from each DEM and a MSGLV ratio was computed using Eq. (1):

$$\text{MSGLV ratio} = \text{Edge MSGLV}/\text{Internal MSGLV}. \tag{1}$$

The MSVLV ratio is a relative measure and attempts to quantify how well land component boundaries coincide with morphological discontinuities.

Table 3
Scale factors and the number of delineated land components for each DEM.

DEM	Scale factor	Total number of LC	% difference of number of LC from GEOEYE DEM LC
ASTER GDEM2	24	21,086	−2.73
GEOEYE DEM	12	21,678	0.0
SUDEM L1	24	21,949	1.25
SUDEM L2	11	21,443	−1.08
SRTM DEM	12	20,670	−4.65

LC — Land components, ASTER GDEM2 — second version of the 30-m advanced spaceborne thermal emission and reflection radiometer global digital elevation model, SRTM DEM — the 90-m shuttle radar topography mission digital elevation model and SUDEM (L1 and L2) — Stellenbosch University digital elevation models (levels 1 and 2).

3. Results and discussion

A subset of the 0.5-m orthorectified digital aerial photograph and land components generated from the five DEMs is depicted in Fig. 4a–f. The GEOEYE DEM, SUDEM L2 and the SRTM DEM land components look similar in shape and are distinctively different from the land components generated from ASTER GDEM2 and SUDEM L1 (Fig. 4a–f). Closer visual inspection revealed that the GEOEYE DEM very effectively identifies morphological discontinuities (i.e. slope gradient and aspect breaks) (Fig. 4b and c). Land component boundaries delineated from the GEOEYE DEM and SUDEM L2 mostly coincided with morphological discontinuities. However, the GEOEYE DEM land components were more sensitive to morphological discontinuities than those of SUDEM L2. The GEOEYE DEM land components yielded more detailed morphological discontinuities and incorporated land surface features (for example trees and buildings) in certain areas. This is very likely due to the way the DEMs were created. The GEOEYE DEM was created from stereo-imagery whereas the SUDEM L2 was created from large-scale contour data fused with the SRTM DEM. Consequently, the GEOEYE DEM is a more detailed DEM than the SUDEM L2. The reason why the GEOEYE DEM incorporated land surface features in the delineation in certain areas is because it is a surface model as opposed to the SUDEM L2, which is a terrain model. Despite the SRTM DEM land components looking similar in shape to those of the GEOEYE DEM and SUDEM L2, they were less sensitive to morphological discontinuities. Fig. 4d shows that the SRTM DEM land components are generalized in certain areas and do not coincide with some significant morphological discontinuities. This is attributed to the lower native resolution (90 m) of the SRTM DEM. The ASTER GDEM2 and SUDEM L1 also failed to identify many significant morphological discontinuities (Fig. 4e and f). This result confirms those of Gichamo et al. (2012), Frey and Paul (2012) and Shafique et al. (2011) who found that the ASTER GDEM2 quality is dependent on factors such as quality of the image pair, image acquisition angle and terrain complexity. Contour-interpolated DEMs such as the SUDEM L1 are usually not as accurate as DEMs generated by other means, because DEMs generated from contours suffer from oversampling in steep areas and generalizations in flat terrain (Ardiansyah and Yokoyama, 2002; Taud et al., 1999; Vaze et al., 2010; Wise, 2007; Xie et al., 2003).

The GEOEYE DEM and SRTM DEM land components yielded the lowest (1.2) overall (mean) SGSD (Table 4). This suggests that these products are internally the most homogeneous. The low mean SGSD of the SRTM-delineated land components is attributed to the relatively low

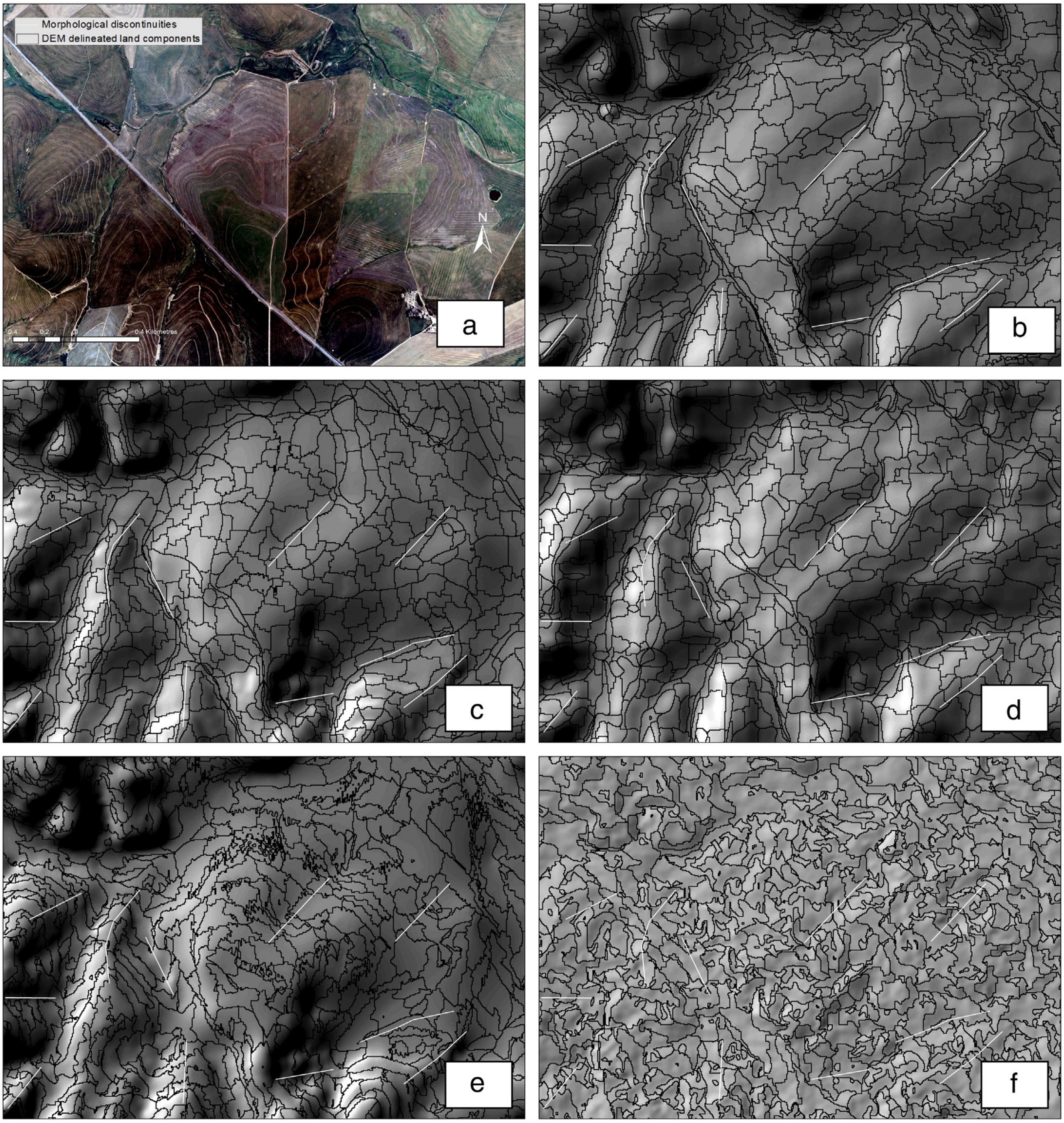

Fig. 4. A detailed view of an area within the Sandspruit catchment represented as an (a) orthorectified digital aerial photograph, compared to land component maps of the same area derived from the (b) GEOEYE DEM, (c) SUDEM L2, (d) SRTM DEM, (e) SUDEM L1 and (f) ASTER GDEM2.

Table 4
Overall SGSDs of digital elevation models.

DEM	Mean SGSD
ASTER GDEM2	4.4
GEOEYE DEM	1.2
SUDEM L1	1.5
SUDEM L2	1.3
SRTM DEM	1.2

ASTER GDEM2 — second version of the 30-m advanced spaceborne thermal emission and reflection radiometer global digital elevation model, SRTM DEM — the 90-m shuttle radar topography mission digital elevation model, SUDEM (L1 and L2) — Stellenbosch University digital elevation models (level 1 and 2), LC — Land components and SGSD — slope gradient standard deviation.

resolution of the SRTM DEM (90 m) which limits the variation within land components. The mean SGSD of the SUDEM L2 product is not significantly higher (1.3) than those of the GEOEYE DEM and SRTM DEM. The ASTER GDEM2 land components are the least homogeneous internally (mean SGSD of 4.4). The histogram of SGSD (Fig. 5) revealed that, in contrast to the other DEMs, most of the ASTER GDEM2 land components are highly heterogeneous in terms of slope gradient. This result suggests that the ASTER GDEM2 is not suitable for land component mapping.

The internal MSGLV for the GEOEYE DEM, SUDEM L2, SRTM DEM and ASTER GDEM2 were lower than the edge MSGLV, resulting in a MSGLV ratio of more than 1 (Table 5). This indicates that the internal homogeneity of the land components delineated from these DEMs is maximized, while the homogeneity at the edges is minimized and consequently suggests that land component boundaries coincide with

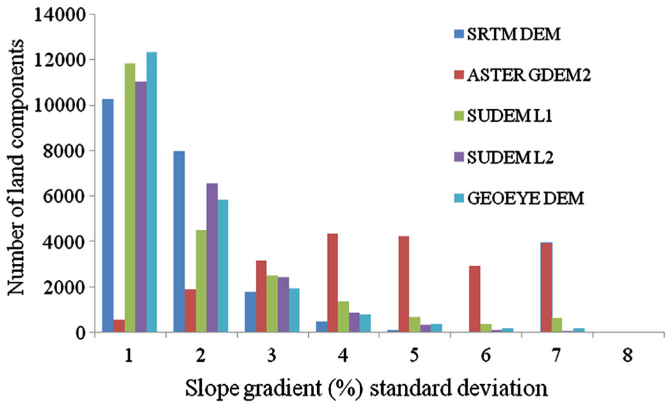

Fig. 5. Mean slope gradient (%) standard deviation of the land components delineated from different DEMs.

morphological discontinuities. In contrast, the internal and external MSGLV for the SUDEM L1 land components are equal (MSGLV ratio is 1), indicating that morphological discontinuities are not effectively represented by land component boundaries. GEOEYE DEM and SUDEM L2 yielded land components with the highest MSGLV ratio and as such are the most successful in representing terrain transitions. This was confirmed during the visual inspection of the land component boundaries, which revealed that these two DEMs perform equally well in producing land components boundaries that coincide with morphological discontinuities. The high accuracy of delineated land components from SUDEM L2 was unexpected given that SUDEM L1 and SRTM DEM (which was used to develop the SUDEM L2) did not perform as well. This result seems to suggest that the way in which 5-m vertical contour data and spot heights were fused with the SRTM DEM in areas of moderate terrain (i.e. where the density of contours is low) optimizes the detail of each input DEM (Van Niekerk, 2011).

In spite of its relatively lower MSGLV, the SRTM DEM outperformed the ASTER GDEM2 regarding the identification of morphological discontinuities as evidenced by visual inspection and the SGSD. This finding is consistent with that of Frey and Paul (2012) who found that SRTM DEM yielded slightly accurate results than ASTER GDEM for the compilation of topographic parameters in glacier inventories. Siart et al. (2009) concluded that, despite its coarser resolution, SRTM DEM yielded more satisfactory results than ASTER GDEM for identifying large depressions.

4. Conclusions

This study compared land components delineated from five different DEMs. The GEOEYE DEM (created from GeoEye stereo-images) was the most effective in producing land component boundaries that coincide with morphological discontinuities. The SUDEM L2 (created from contours and SRTM data) produced similar land components to those of the GEOEYE DEM, and it was almost as successful in maximizing internal (interclass) homogeneity and minimizing external (intraclass) homogeneity. The SRTM DEM appeared to be more suitable for land component mapping than the ASTER GDEM2.

A novel measure, namely the MSGLV ratio, was developed and applied in this study for evaluating how well land component boundaries coincide with morphological discontinuities. The MSGLV ratio measures the relationship between internal homogeneity and external heterogeneity of land components. The ratio complimented the other validation techniques used.

In this research slope gradient and slope aspect was used as input to segmentation. More research is needed to determine how other DEM derivatives (e.g. plan curvature and profile curvature) can effectively be combined in MRS to improve land component delineation and accuracy assessment.

The research demonstrated that a DEM's properties (e.g. resolution, source data, and development method) have significant impacts on the delineation of land components. This has decisive implications for all applications using land components. An example of such an affected application is digital soil mapping which relies on the principle of a strong relationship between terrain and soil properties, and that soil boundaries coincide with land component boundaries. Discrepancies between land component boundaries and terrain transitions will consequently lead to unreliable deductions and inaccurate soil maps.

Table 5
Land component internal and edge MSGLV for each digital elevation model.

DEM	Internal MSGLV	Edge MSGLV	MSGLV Ratio
ASTER GDEM2	1.9	2.4	1.3
GEOEYE DEM	0.6	0.9	1.5
SUDEM L1	0.6	0.6	1.0
SUDEM L2	0.6	0.8	1.5
SRTM DEM	0.5	0.7	1.3

MSGLV — mean slope gradient local variance, ASTER GDEM2 — second version of the 30-m advanced spaceborne thermal emission and reflection radiometer global digital elevation model, SRTM DEM — the 90-m shuttle radar topography mission digital elevation model and SUDEM (L1 and L2) — Stellenbosch University digital elevation models (levels 1 and 2).

Acknowledgments

The Water Research Commission, National Research Foundation and the Agricultural Research Council-Institute for Soil, Climate and Water, are thanked for funding this work. The Chief Directorate National Geo-spatial Information is acknowledged for providing the digital aerial images. We express our appreciation to Dr. Pieter de Necker for editing the manuscript.

References

Adediran, A.O., Parcharidis, I., Poscolieri, M., Pavlopoulos, K., 2004. Computer-assisted discrimination of morphological units on north-central Crete (Greece) by applying multivariate statistics to local relief gradients. Geomorphology 58, 357–370.
Ardiansyah, P.O.D., Yokoyama, R., 2002. DEM generation method from contour lines based on the steepest slope segment chain and a monotone interpolation function. ISPRS J. Photogramm. Remote Sens. 57, 86–101.
Argialas, D.P., 1995. Towards structured-knowledge models for landform representation. Z. Geomorphol. N.F. 101, 85–108.
ASTER GDEM Validation Team, 2011. [Online]. Available http://www.gdem.aster.ersdc.or.JP (Date accessed: 20 July 2011).
Behrens, T., Zhu, A.-X., Schmidt, K., Scholten, T., 2010. Multi-scale digital terrain analysis and feature selection for digital soil mapping. Geoderma 155, 175–185.
Blaschke, T., 2010. Object based image analysis for remote sensing. ISPRS J. Photogramm. Remote Sens. 65, 2–16.
Blaschke, T., Stobl, J., 2003. Defining landscape units through integrated morphometric characteristics. In: Buhmann, E., Ervin, S. (Eds.), Landscape Modeling: Digital Techniques for Landscape Architecture. Wichmann Verlag, Heidelberg, pp. 104–113.
CGIAR-CSI, 2011. . [Online]. Available http://srtm.csi.cgiar.org (Date accessed: 20 July 2011).
Deng, Y., 2007. New trends in digital terrain analysis: landform definition, representation, and classification. Prog. Phys. Geogr. 31, 405–419.
Drăguţ, L., Blaschke, T., 2006. Automated classification of landform elements using object-based image analysis. Geomorphology 81, 330–344.
Drăguţ, L., Eisank, C., 2011. Object representations at multiple scales from digital elevation models. Geomorphology 129, 183–189.
Drăguţ, L., Tiede, D., Levick, S.R., 2010. ESP: a tool to estimate scale parameter for multiresolution image segmentation of remotely sensed data. Int. J. Geogr. Inf. Sci. 24, 859–871.
Drăguţ, L., Eisank, C., Strasser, T., 2011. Local variance for multi-scale analysis in geomorphometry. Geomorphology 130, 162–172.
Farr, T.G., 2000. The shuttle radar topography mission. IEEE Aerospace Conference Proceedings, p. 63.
Farr, T., Kobrick, M., 2001. The shuttle radar topography mission. Am. Geophys. Union EOS 81, 583–585.
Flügel, W.A., 1995. River salinity due to dryland agriculture in the Western Cape Province, Republic of South Africa. Environ. Int. 21, 679–686.
Frey, H., Paul, F., 2012. On the suitability of the SRTM DEM and ASTER GDEM for the compilation of topographic parameters in glacier inventories. Int. J. Appl. Earth Obs. Geoinf. 18, 480–490.

Gichamo, T.Z., Popescu, I., Jonoski, A., Solomatine, D., 2012. River cross-section extraction from the ASTER global DEM for flood modeling. Environ. Model. Softw. 31, 37–46.
Graff, L.H., Usery, E.L., 1993. Automated classification of generic terrain features in digital elevation models. Photogramm. Eng. Remote. Sens. 59, 1409–1417.
Jenny, H., 1941. Factors of Soil Formation. McGraw-Hill, New York.
Li, J., Wong, D.W.S., 2010. Effects of DEM sources on hydrologic applications. Comput. Environ. Urban Syst. 34, 251–261.
MacMillan, R.A., Jones, R.K., McNabb, D.H., 2004. Defining a hierarchy of spatial entities for environmental analysis and modeling using digital elevation models (DEMs). Comput. Environ. Urban Syst. 28, 175–200.
Mancas, M., Gosselin, B., Macq, B., 2005. Segmentation using a region-growing thresholding. Proceedings of the Electronic Imaging Conference of the International Society for Optical Imaging (SPIE/EI 2005), San Jose, USA.
Mathieu, R., Freeman, C., Aryal, J., 2007. Mapping private gardens in urban areas using object-oriented techniques and very high-resolution satellite imagery. Landsc. Urban Plan. 81, 179–192.
McBratney, A.B., Mendonca Santos, M.L., Minasny, B., 2003. On digital soil mapping. Geoderma 117, 3–52.
Minár, J., Evans, I.S., 2008. Elementary forms for land surface segmentation: the theoretical basis of terrain analysis and geomorphological mapping. Geomorphology 95, 236.
Moller, M., Volk, M., Friederich, K., Lymburner, L., 2008. Placing soil genesis and transport processes into landscape context: a multiple terrain analysis approach. J. Plant Nutr. Soil Sci. 171, 419–430.
Mukherjee, S., Joshi, P.K., Mukherjee, S., Ghosha, A., Garg, R.D., Mukhopadhyyaya, A., 2013. Evaluation of vertical accuracy of open source Digital Elevation Model (DEM). Int. J. Appl. Earth Obs. Geoinf. 21, 205–217.
Mulder, V.L., De Bruin, S., Schaepman, M.E., Mayr, T.R., 2011. The use of remote sensing in soil and terrain mapping — a review. Geoderma 162, 1–19.
Rodriguez, E., Morris, C.S., Belz, J.E., Chaplin, E.C., Martin, J.M., Daffer, W., Hensley, S., 2005. An Assessment of the SRTM Topographic Products. Jet Propulsion Laboratory, Pasadema.
Shafique, M., van der Meijde, M., Kerle, N., van der Meer, F., 2011. Impact of DEM source and resolution on topographic seismic amplification. Int. J. Appl. Earth Obs. Geoinf. 13, 420–427.
Siart, C., Bubenzer, O., Eitel, B., 2009. Combining digital elevation data (SRTM/ASTER), high resolution satellite imagery (Quickbird) and GIS for geomorphological mapping: a multi-component case study on Mediterranean karst in Central Crete. Geomorphology 112, 106–121.
Smith, G., Beare, M., Boyd, M., Downs, T., Gregory, M., Morton, D., Brown, N., Thompson, A., 2007. Land cover map production through generalization of OS mastermap. Cartogr. J. 44, 276–283.
Speight, J.G., 1977. Landform pattern description from aerial photographs. Photogrammetria 32, 161–182.
Taud, H., Parrot, J.-F., Alvarez, R., 1999. DEM generation by contour line dilation. Comput. Geosci. 25, 775–783.
Thakur, A., Anand, R.S., 2005. The local statistics based region growing segementation method for ultrasound medical images. Int. J. Signal Process. 1, 141–146.
Thompson, J.L., Bell, J.C., Butler, C.A., 2001. Digital elevation model resolution: effects on terrain attribute calculation and quantitative soil-landscape modelling. Geoderma 100, 67–89.
Trimble, 2011. eCcognition Developer 8.64.1 Reference Book. Tribmle Germany GmbH, Munich.
van Asselen, S., Seijmonsberen, A.C., 2006. Expert-driven semi-automated geomorphological mapping for a mountainous area using a laser DTM. Geomorphology 78, 309–320.
Van Niekerk, A., 2008. CLUES: A Web-Based land Expert System for the Western Cape. (Doctoral dissertation) Stellenbosch University, Stellenbosch.
Van Niekerk, A., 2010. A comparison of land unit delineation techniques for land evaluation in the Western Cape, South Africa. Land Use Policy 27, 937–945.
Van Niekerk, A., 2011. Stellenbosch University Digital Elevation Model Product Description, 2011 edition. Centre for Geographical Analysis, Stellenbosch.
Van Niekerk, A., 2012. Developing a High Resolution DEM of South Africa. Position IT, pp. 55–60 (November–December).
Vaze, J., Teng, J., Spencer, G., 2010. Impact of DEM accuracy and resolution on topographic indices. Environ. Model. Softw. 25, 1086–1098.
Wise, S.M., 2007. Effect of differing DEM creation methods on the results from a hydrological model. Comput. Geosci. 33, 1351–1365.
Wulder, M.A., White, J.C., Hay, G.J., Castilla, G., 2008. Pixels to objects to information: spatial context to aid in forest characterization with remote sensing. In: Blaschke, T., Lang, S., Hay, G.J. (Eds.), Object-Based Image Analysis. Spatial Concepts for Knowledge-Driven Remote Sensing Applications. Springer, Heidelberg, Berlin, pp. 345–363.
Xie, K., Wu, Y., Ma, X., Liu, Y., Liu, B., Hessel, R., 2003. Using contour lines to generate digital elevation models for steep slope areas: a case study of the Loess Plateau in North China. Catena 54, 161–171.